Available online at website: https://journal.bcrec.id/index.php/bcrec

Bulletin of Chemical Reaction Engineering & Catalysis, 19 (2) 2024, 300-317

Research Article

New Modeling Approaches for Ethylene Oxychlorination in Fluidized Bed Reactors: Industrial and Low Flow Rate Conditions

Wail El Bazi [1*], Mustapha Bideq [2], Abderrahim El-Abidi [2], Said Yadir [2]

[1]*Laboratory of Process Engineering, Computer Science and Mathematics, Department of Process Engineering, National School of Applied Sciences of Khouribga, Sultan Moulay Slimane University, Bd Béni Amir, BP 77, 25000, Khouribga, Morocco*

[2]*Laboratory of Materials, Processes, Environment and Quality (LMPEQ), National School of Applied Sciences of Safi, Cadi Ayyad University, Route Sidi Bouzid BP 63, 46000 Safi, Morocco.*

Received: 24th April 2024; Revised: 21th June 2024; Accepted: 23th June 2024
Available online: 27th June 2024; Published regularly: August 2024

Abstract

A simple model (Continuous Stirred-Tank Reactor) has been developed to predict the behavior of industrial ethylene oxychlorination fluidized beds operating in a turbulent regime. The approach showed good agreement both with results from industrial reactors and with those corresponding to the (Simple two phases-Plug bubble-Mixed flow emulsion approach) validated in the literature. For low flow rates, the use of the (Simple two phases - Plug bubble - Plug emulsion model) adapted to these conditions enabled us to highlight the location and extent of undesirable thermal hot spots for the process, and to propose actions to control them by acting on the temperature and/or on the feed gas flows. By comparing this model with the plug approach, the significant slowdown in ethylene conversion caused by resistance to mass transfer when feed flow rates are low is highlighted.

Keywords: Fluidized bed reactor; Bubble phase; Emulsion phase; Continuous Stirred Tank Reactor; Plug Reactor

How to Cite: W. El Bazi, M. Bideq, A. El-Abidi, S. Yadir (2024). New Modeling Approaches for Ethylene Oxychlorination in Fluidized Bed Reactors: Industrial and Low Flow Rate Conditions. *Bulletin of Chemical Reaction Engineering & Catalysis*, 19 (2), 300-317 (doi: 10.9767/bcrec.20148)

Permalink/DOI: https://doi.org/10.9767/bcrec.20148

1. Introduction

1,2-Dichloroethane is used as a pesticide, degreaser and paint stripper, as well as an additive solvent to improve the octane rating of gasoline [1], but its primary use is in the synthesis of polyvinyl chloride, which is involved in the manufacture of thermoplastics [2] found in pipes, wall coverings, window frames, vinyl seat covers and many other everyday products [3]. The 1,2-Dichloroethane can be obtained either by direct chlorination or by oxychlorination [4]. The first process is carried out in the liquid phase and in the presence of a homogeneous ferric chloride catalyst [4], while the second takes place in the gas phase in the presence of a solid alumina-supported copper chloride catalyst [5], whose role is to avoid friction and ensure better surface control [6]. Oxychlorination takes place by reacting ethylene with chloridric acid and oxygen (pure or contained in the air) to produce 1,2-dichloroethane and water, based on the chemical reaction:

$$C_2H_4 + 0.5O_2 + 2HCl \rightarrow CH_2CH_2Cl_2 + H_2O$$

On an industrial scale, this reaction takes place at temperatures of 200 to 300 °C and pressures of 1 to 10 bar [5]. Oxychlorination is highly exothermic ($\Delta H_{r,298K}$ = -295 kJ.mol^{-1}), hence the need for temperature control to ensure the success of the process. Temperatures exceeding 400 °C lead to sublimation of the catalyst [2], and

* Corresponding Author.
Email: w.elbazi@usms.ma (W. El Bazi)

even above 240 °C, competitive reactions occur, giving rise to several by-products (C_2Cl_3HO, CO, CO_2, C_2H_5Cl, $C_2H_3Cl_3$, … etc.), which reduces the selectivity of 1,2-dichloroethane formation [5]. To prevent excessive temperature rises and reach a thermal profile close to isothermicity, the fluidized-bed reactor remains a good alternative [7]. This technology, which has been used in industry for over a century [6], is the most widely adopted for large-scale ethylene oxychlorination [3,5,6-8]. In addition to temperature control, this technology offers the advantage of overcoming the resistance to material transfer present in fixed-bed reactors, which causes a significant slowdown in the apparent reaction rate [9,10].

For more accurate prediction of the behavior, diagnosis, design and optimization of fluidized bed operation, modeling and simulation are highly reliable tools. The literature offers a wide range of one-dimensional models for predicting the behavior of these converters. Models range from the simplest, based on the assumption of an ideal reactor (plug (P) or continuous stirred-tank reactor (CSTR)) with a single phase [11,12], to more complex models taking into account the presence of two phases (bubble, emulsion) or even three phases (bubble, cloud-wake and emulsion). Some of these models consider that each phase has a plug-like behavior, with material and heat transfers between phases (P-P model) [12-15]. Other multiphase models assume that the emulsion behaves like a CSTR reactor, with non-reactive or reactive bubbles behaving like plug (P-M models) [16-18]. Other papers have even proposed multidimensional approaches to study these reactors [19-21].

These models have been well used in the modeling and simulation of fluidized-bed catalytic reactors for ethylene oxychlorination on an industrial scale. Montebelli *et al.* [5] developed a single-phase model with axial dispersive plug flow (ADPF) to predict the behavior of these converters. The model takes into account the main reaction and several concurrent secondary ones. The choice of a single-phase model is justified by the fact that, at very high flow rates, the fluidization regime is very fast and, under these conditions, there is no distinction between phases [5]. Some authors suggest that under industrial conditions characterized by high superficial velocities, the emulsion may behave as a CSTR, while the non-reactive bubble behaves as a plug. A well-cited paper in this regard is that by Al-Zahrani *et al.* [7], which focused on a two-phase model based on the above assumptions to simulate the behavior of an industrial converter. Al-Zahrani's model takes into account only the main oxychlorination reaction. Khademi *et al.* [3] have used a model closely similar to Al-Zahrani's, also taking into account only the main reaction, but using different reaction kinetics. Indeed, Al Zahrani used the reaction kinetics developed by Wachi *et al.* which expresses the reaction kinetics as a function of ethylene concentration, copper concentration in the catalyst, and temperature [22], whereas the kinetics used by Khademi *et al.* is the one developed by Carrubba *et al.* [23], expressing the reaction rate as a function of the partial pressures of ethylene, oxygen, water vapour, and temperature. Other studies have used the same model (P-M model), but taking into account secondary reactions in addition to the main one [5,6,24]. The 3-phase models have also been used to study these industrial reactors. With this in mind, Faghih *et al.* [8] developed a model (bubble-cloud-emulsion) to predict ethylene conversion at the outlet of an industrial oxychlorination reactor. The kinetic expression embedded in the model takes into account the main reaction and the parasitic reactions leading to the formation of CO and CO_2. Another study has investigated the behavior of these reactors in 3D using CFD based on an Eulerian-Eulerian flow model [25] where only the main reaction had been taken into account.

Although the models presented were able to provide a good approximation to the behavior of industrial converters, many of them present certain mathematical difficulties for solving them. For example, the (P-M model) with non-reactive bubbles requires the resolution of a system comprising a number of non-linear equations, which is increasingly important if we take into account more and more concurrent reactions [3,6,7,16,17]. Moreover, these models have not covered all the assumptions that can be justified in the case of industrial converters, where feeding takes place at very high flow rates. Among these assumptions, the behavior of the fluidized bed is considered as a single-phase continuous stirred reactor. Indeed, in the turbulent regime, single-phase models can adequately describe the behavior of fluidized beds [26]. It has even been shown that under relatively high superficial velocity conditions, the single-phase continuous stirred reactor approach correctly describes the evolution of temperatures and concentrations in industrial polyethylene fluidized bed reactors [11]. The study by Toei *et al.* [27] of ethylene hydrogenation in a fluidized bed reactor revealed that the CSTR approach provides an acceptable estimation of the hydrogen conversion at high superficial velocities. Therefore, given that EDC cracking in fluidized beds occurs in turbulent regime, and then, at superficial velocities several times higher than the minimum fluidization velocity [5,6], the CSTR hypothesis is worthy to be evaluated. For this reason, we have developed a simple CSTR model to predict the behavior of these industrial converters. The results obtained

using this model were compared to experimental results from the literature corresponding to several industrial reactors [3,5,7]. A parametric sensitivity analysis was carried out to evaluate the effect of several key parameters (pressure, feed temperature, cooling temperature, feed molar distribution) on reactor behavior under industrial conditions. The curves obtained from this analysis were compared with the numerical simulation results corresponding to the (P-M model) from previous studies based on this approach [3,7]. In fact, the CSTR approach offers the advantage of ease of implementation and ease of mathematical resolution. Indeed, if there is only one reaction in the converter, it is sufficient to solve a system of two non-linear equations corresponding to the material balance and the energy balance in the reactor. Validation of this approach for industrial fluidized beds for ethylene oxychlorination will enable the behavior of these plants to be predicted without having to resort to more numerically complex models.

In addition to industrial situations, characterized by a turbulent regime, it is also important to predict the behavior of these fluidized beds when the superficial velocity is not very high. This is often the case in laboratory reactors [2], or when the pilot operates at low flow rates. Given that modeling and simulation work in the literature has focused solely on the study of these installations under industrial conditions characterized by high gas flows, hence the presence of back-mixing justifying the adoption of CSTR or P-M models, the case of low superficial velocities ($U_0 \leqslant 6U_{mf}$) was also evaluated. Under these conditions, it is more appropriate to use a (P-P model) [14,28]. In fact, plug flow for the bubble is still valid [14], while for the emulsion phase, this type of flow is reasonable where the superficial velocity is low given the absence of catalyst back-mixing under these conditions. The second part of this paper therefore focuses on exploiting this approach to evaluate the behavior of these converters in such circumstances. By means of these simulations, we were able to predict the location and magnitude of thermal hot spots with disastrous effects on the catalyst and on the selectivity of 1,2-dichloroethane [2,5,6,29], and thus propose solutions to attenuate them. These simulations also enabled us to evaluate the importance of limitations to heat transfer between phases, by determining the thermal profile in the bubbles and in the emulsion. Finally, a comparison of the (P-P model) with the (P model) made it possible to measure the impact of interphase material transfer resistances on ethylene conversion at low gas flow rates.

2. Modeling Methods and Numerical Solutions

The calculation code used to solve this problem has been developed under Matlab software.

2.1 Fluidized Bed Assumptions and Calculation of Hydrodynamic Characteristics and Transport Properties

For the studied models, we have assumed that the bubble is free of solids and that the entire catalytic mass is located in the emulsion, so the reaction takes place exclusively in this phase. This assumption can be justified by the small size of the catalytic grains considered in the simulations [30]. The emulsion phase is also assumed to be at the fluidization minimum, regardless of superficial velocity. Finally, we neglect the resistance to transfer phenomena between this phase and the solid, which can be justified by the extreme rapidity of these phenomena between the two phases [5].

The correlations for calculating the hydrodynamic characteristics and transport properties of the fluidized bed are presented in Table 1. The expressions concerning the viscosities μ_i and conductivities λ_i of different elements with respect to temperature were taken from reference [35]. The formula for calculating binary diffusion coefficients $D_{(i,j)}$ can be found in [7].

2.2 Continuous Stirred Reactor Model (CSTR Model)

When modeling the fluidized-bed converter as a continuous stirred reactor, it has been assumed that the converter behaves as a single-phase reactor with uniform catalyst distribution [32]. The equation corresponding to the material balance depends on the limiting reactant:
If ethylene is the limiting reactant:

$$F_{C2H4,0} - F_{C2H4} + \alpha_{C2H4}.r_{C2H4Cl2}.S.L.\left(1-\varepsilon_{moy}\right) = 0 \quad (21)$$

If chloridric acid is the limiting reactant:

$$F_{HCl,0} - F_{HCl} + \alpha_{HCl}.r_{C2H4Cl2}.S.L.\left(1-\varepsilon_{moy}\right) = 0 \quad (22)$$

$F_{i,0}$ and F_i correspond to the molar flow rates of component i in mol.s^{-1} at the inlet and outlet of the converter, α_i refers to the stechiometric coefficient of component i (negative for reactants, positive for products and zero for elements not involved in the reaction), $r_{C2H4Cl2}$ (mol.s^{-1}.m^{-3}) is the reaction rate for the production of 1,2-dichloroethane which is given by the equation:

$$r_{C2H4Cl2} = \frac{K_r.K_a.C_C.C_E}{1+K_a.C_E} \quad (23)$$

with K_r (s^{-1}) is the rate constant:

$$K_r = 269.exp\left(\frac{-E_a}{R_g.T}\right) \quad (24)$$

E_a is the activation energy (37,800 $J.mol^{-1}$), R_g is the gas constant (8,314 $J.mol^{-1}.K^{-1}$), T(K) is the bed temperature, K_a is the adsorption equilibrium constant (0.63 $m^3.mol^{-1}$), C_c ($mol.m^{-3}$) is the copper concentration in the catalyst, and C_E ($mol.m^{-3}$) is the ethylene concentration. The reaction kinetics used corresponds to that of Wachi *et al.* [22]. The expression of the ethylene concentration depends on the limiting reactant. If ethylene is the limiting reactant:

$$C_{C2H4} = \frac{F_{0,C2H4}.(1-X_{C2H4})}{Q_0\frac{P_0.T}{P.T_0}(1+\varepsilon_{C2H4}.X_{C2H4})} \quad (25)$$

Q_0 (m^3) is the volume flow feeding the reactor ($Q_0 = \frac{\left(\sum_{i=1}^{i=N} F_{i,0}\right).R_g.T_0}{P_0}$) , T_0 (K) is the feed temperature, and P_0 (Pa) is the reactor inlet pressure.

The chemical expansion factor corresponding to ethylene (ε_{C2H4}) is calculated by equation:

$$\varepsilon_{C2H4} = \frac{-1.5.F_{0,C2H4}}{F_{T,0}} \quad (26)$$

With $F_{T,0}$ ($mol.s^{-1}$) is the total molar flow rate feeding the reactor ($F_{T,0} = \sum_{i=1}^{i=N} F_{i,0}$).

If hydrochloric acid is the limiting reactant:

$$C_{C2H4} = \frac{F_{0,C2H4}.-0.5.F_{0,HCl}.X_{HCl}}{Q_0\frac{P_0.T}{P.T_0}(1+\varepsilon_{HCl}.X_{HCl})} \quad (27)$$

The expansion factor corresponding to chloridric acid (ε_{HCl}) is expressed by the formula:

$$\varepsilon_{HCl} = \frac{-0.75.F_{0,HCl}}{F_{T,0}} \quad (28)$$

X_j ($X_j = \frac{F_{j,0}-F_j}{F_{j,0}}$) being the conversion of reactant j, S (m^2) is the reactor cross-sectional area, and L (m) is the expanded bed height and ε_{moy} corresponds to the average voidage of the reactor. The formulas required to calculate L and ε_{moy} are shown in Table 1. Meanwhile, the energy balance in the installation yields equation [36]:

$$m_{mix}.C_{p,mix}(T_0).\left(T_0 - T_{ref}\right) - h_w.\pi.D.L.(T - T_w) - \Delta H_r.r_{C2H4Cl2}.S.L.\left(1 - \varepsilon_{moy}\right) - m_{mix}.C_{p,mix}(T).(T - T_{ref} \quad (29)$$

m_{mix} ($kg.s^{-1}$) is the mass flow rate of the gas mixture feeding the reactor, which is calculated by adopting the equation:

$$m_{mix} = \sum_{i=1}^{i=N} F_i.M_i \quad (30)$$

$C_{p,mix}$(T) is the specific heat capacity ($J.kg^{-1}.K^{-1}$) of the gas mixture at reactor temperature, which is expressed with the formula:

$$C_{p,mix}(T) = \frac{\sum_{i=1}^{i=N} y_i.C_{p,i}(T)}{M_{mix}} \quad (31)$$

$C_{p,i}$(T) correspond to the heat capacities ($J.mol^{-1}.K^{-1}$) of the different elements i. Expressions for these capacities as a function of temperature are available in [35], y_i is the mole fraction of element i in the mixture ($y_i = \frac{F_i}{\sum_{i=1}^{i=N} F_i}$) and M_i ($kg.mol^{-1}$) is its molecular weight. T_{ref} is the reference temperature of 298 K, h_w ($W.m^{-2}.K^{-1}$) is the overall heat-transfer coefficient between the wall and the fluidized bed, calculated as shown in Table 1, D (m) is the reactor diameter, T_W (K) is the catalytic bed wall temperature and ΔH_r ($J.mol^{-1}$) is the enthalpy of reaction, calculated as shown in [37]. The systems of non-linear equations ((21); (29)) and ((22) ; (29)) are solved by the Newton-Raphson method [38] (Figure S1 Supporting Information).

2.3. Plug Model (P Model)

As with the continuous stirred reactor, we assume single-phase behavior and that the solid is uniformly distributed in the reactor with an average voidage ε_{moy}, calculated in the same way as for the CSTR average voidage. The mass balance along the reactor leads to the differential equation:

$$\frac{dX_i}{dZ} = \frac{r_{C2H4Cl2}.S.\left(1-\varepsilon_{moy}\right)}{F_{0,i}} \quad (32)$$

The heat balance leads to the differential equation:

$$\frac{dT}{dZ} = \frac{-\Delta H_r.r_{C2H4Cl2}.\left(1-\varepsilon_{moy}\right).S - h_w.\pi.D.L.(T(Z)-T_w)}{\sum_{i=1}^{i=N} F_i.C_{p,i}(T)} \quad (33)$$

To take into account the pressure drop along the installation, we adopt equation [26]:

$$\frac{dP}{dZ} = -g.\rho_p.(1 - \varepsilon_{moy}) \quad (34)$$

where, P is the pressure (Pa), g is the acceleration of gravity ($9.81.m.s^{-2}$) and ρ_p ($kg.m^{-3}$) is the density of the catalyst. The system of ordinary differential equations in Equations (32)-(34) can be solved by the Runge-Kutta 4 method [9,10] with the following initial conditions at reactor inlet: X_i=0, T=T_0, P=P_0.

2.4. Simple Two-Phase Model – Plug Emulsion-Plug Bubble (P-P Msodel)

This model assumes the existence of two phases in the reactor: a bubble phase and an emulsion phase. Each of the two phases is characterized by a plug behavior, with mass and heat transfer between both [14,39]. Since the bubble phase contains no catalyst, the mass balance in this phase leads to the equation:

$$\frac{dN_{i,b}}{dZ} = K_i.S.\delta.\left(\frac{N_{i,e}(Z)}{Q_e(Z)} - \frac{N_{i,b}(Z)}{Q_b}\right) \quad (35)$$

δ is the volume fraction of bubble phase to overall bed, calculated as shown in Table 1, $N_{i,b}$ and $N_{i,e}$ (mol.s^{-1}) are respectively the molar flow rates of element i in the bubble and emulsion phases, K_i (s^{-1}) is the overall mass-transfer coefficient (bubble phase–emulsion phase) based on bubble volume (s^{-1}), calculated as shown in Table 1, Q_b and Q_e in m^3.s^{-1} refer to the volumetric flow rates

Table 1. Hydrodynamic and transport property correlations

Parameter	Correlation	
Viscosity of gas mixture (Pa.s) [31]	$\mu_{mix} = \sum_{i=1}^{N} \frac{y_i \mu_i}{\sum_{j=1}^{N} y_j \sqrt{\frac{M_j}{M_i}}}$	(1)
Bed voidage at minimum fluidization [7]	$\varepsilon_{mf} = 0.586.\left(\frac{{\mu_{mix}}^2}{\rho_g.g.{d_p}^3.(\rho_p-\rho_g)}\right)^{0.029}.\left(\frac{\rho_g}{\rho_p}\right)^{0.021}$	(2)
Inlet superficial velocity (m.s^{-1})	$U_0 = \frac{Q_0}{S}$	(3)
Superficial velocity at minimum fluidization (m.s^{-1}) [3]	$U_{mf} = \frac{g.{d_p}^2.(\rho_p-\rho_g).{\varepsilon_{mf}}^3}{150.\mu_{mix}.(1-\varepsilon_{mf})}$	(4)
Bubble diameter (m) [18]	$d_b = d_{bm} - (d_{bm} - d_{b0}).exp\left(\frac{-0.15.L_{mf}}{D}\right)$	(5)
Bubble rising velocity (m.s^{-1})) [18]	Where: $d_{b0} = 0.376.\left(U_0 - U_{mf}\right)^2$ $d_{bm} = 1.6377.\left(S.(U_0 - U_{mf})\right)^{0.4}$ $U_b = \left(U_0 - U_{mf}\right) + 0.711.(g.d_b)^{0.5}$	(6)
Volume fraction of bubble phase to overal bed [30]	With: U_br=0.711.⟦(g.d_b)⟧$^{0.5}$	(7)
Expanded bed height (m) [3]	$\delta = \frac{U_0 - U_{mf}}{U_b - U_{mf}}$	(8)
Average voidage of the bed [32]	$L = \frac{L_{mf}}{1-\delta}$	(9)
	$\varepsilon_{moy} = (1-\delta).\varepsilon_{mf}$	(10)
Gas mixture conductivity (W.m^{-1}.K^{-1}) [31]	$\lambda_{g,mix} = \frac{\sum_i \lambda_i y_i \sqrt[3]{M_i}}{\sum_i y_i \sqrt[3]{M_i}}$	(11)
Heat transfer coefficient between wall and bed (W.m^{-2}.K^{-1}) [7]	$h_w = 0.88.\left(\frac{\lambda_{g,mix}}{d_p}\right).\left(\frac{\rho_g.(\rho_p-\rho_g).g.{d_p}^3}{{\mu_{mix}}^2}\right)^{0.213}$	(12)
Diffusivity of component i in gas mixture (m^2.s^{-1}) [7]	$D_{i,mix} = (1-y_i).\left(\sum_{j=1,i\neq j}^{N} \frac{y_i}{D_{i,j}}\right)^{-1}$	(13)
Overall mass-transfer coefficient (bubble phase–emulsion phase) based on bubble volume (s^{-1}) [14]	$K_{bc,i} = 4.5\left(\frac{U_{mf}}{d_b}\right) + 5.85\left(\frac{{D_{i,mix}}^{0.5} g^{0.25}}{{d_b}^{1.25}}\right)$	(14)
	$K_{ce,i} = 6.78.\left(\frac{\varepsilon_{mf}.D_{i,mix}.U_b}{{d_b}^3}\right)^{0.5}$	(15)
	$K_i = \left(\left(\frac{1}{K_{bc,i}}\right) + \left(\frac{1}{K_{ce,i}}\right)\right)^{-1}$	(16)
Overall heat-transfer coefficient (bubble-dense phase) based on bubble volume (W.m^{-3}.K^{-1}) [33]	$H_{bc} = 4.5.\left(\frac{U_{mf}.\rho_g.C_{p,mix}}{d_b}\right) + 5.85\left(\frac{\lambda_{g,mix}.\rho_g.g^{0.5}.C_{p,mix}}{{d_b}^{2.5}}\right)^{0.5}$	(17)
	$H_{ce} = 6.77.\left(\frac{\lambda_{g,mix}.\rho_g.\varepsilon_{mf}.C_{p,mix}.U_{br}}{{d_b}^3}\right)^{0.5}$	(18)
	$H_{be} = \left(\left(\frac{1}{H_{bc}}\right) + \left(\frac{1}{H_{ce}}\right)\right)^{-1}$	(19)
Minimum bubbling velocity (m.s^{-1}) [34]	$U_{mb} = \frac{2300.U_{mf}.{\rho_g}^{0.126}.{\mu_{mix}}^{0.523}}{{d_p}^{0.8}.g^{0.934}.(\rho_p-\rho_g)^{0.934}}$	(20)

in the two phases. To calculate each of the flow rates, we use the equations:
- for the bubble phase:

$$Q_b = U_b.\delta.S \quad (36)$$

U_b (m.s^{-1}) is the bubble rising velocity, calculated as shown in Table 1.

- for the emulsion phase:

$$Q_e(Z) = \frac{(\sum_{i=1}^{i=N} N_{i,e}(Z)).R_g.T_e(Z)}{P(Z)} \quad (37)$$

T_e (K) is the emulsion temperature. The heat balance in the bubble phase leads to the equation:

$$\frac{dT_b}{dZ} = \frac{H_{be}.(T_e(Z)-T_b(Z))}{U_b.\rho_g.C_{p,mix}} \quad (38)$$

H_{be} (W.m^{-3}.K^{-1}) is the overall heat-transfer coefficient (bubble-dense phase) based on bubble volume, calculated as shown in Table 1, where T_b (K) is the temperature of the bubble phase and ρ_g (kg.m^{-3}) is the density of the gas mixture ($\rho_g = \frac{P}{RT}\sum_{i=1}^{i=n} y_i M_i$). Setting up the mass balance in the emulsion phase leads to the equation:

$$\frac{dN_{i,e}}{dZ} = \alpha_i.(1-\delta).\left(1-\varepsilon_{mf}\right).r_{C2H4Cl2}.S. - K_i.S.\delta.\left(\frac{N_{i,e}(Z)}{Q_e} - \frac{N_{i,b}(Z)}{Q_b}\right) \quad (39)$$

ε_{mf} is the bed voidage at minimum fluidization, for which the formula is given in Table 1.

The heat balance on the emulsion phase leads to the equation:

$$\frac{dT_e}{dZ} = \frac{-H_{be}.S.\delta.(T_e(Z)-T_b(Z))}{\rho_g.C_{p,mix}.Q_e(Z)} - \frac{h_w.\pi.D.(T_e(Z)-T_w)}{\rho_g.C_{p,mix}.Q_e(Z)} - \frac{\Delta H_r.r_{C2H4Cl2}.(1-\varepsilon_{mf}).(1-\delta).S}{\rho_g.C_{p,mix}.Q_e(Z)} \quad (40)$$

Equation (34) is adopted to determine the pressure drop along the reactor. The system of differential equations in Equations (34-35, 38-40) is also solvable by the Runge-Kutta 4 method with the following initial conditions applied to the reactor inlet:

X_i=0, $T_{e,0}$=$T_{b,0}$=T_0, $N_{ib,0} = \frac{N_{i,0}.Q_b}{(Q_b+Q_{e,0})}$, $N_{ie,0} = \frac{N_{i,0}.Q_{e,0}}{(Q_b+Q_{e,0})}$ and P=P_0.

The conversion of the reactant i is calculated by the equation:

$$X_i(Z) = \frac{F_{i,0}-(N_{i,e}(Z)+N_{i,b}(Z))}{F_{i,0}} \quad (41$$

3. Results and Discussion

3.1. Validation of the CSTR Model under Industrial Conditions

The CSTR model was evaluated under different conditions corresponding to several industrial fluidized bed reactors. Table 2 gives the characteristics and operating conditions of the industrial fluidized bed converters studied. Table 3 provides a comparison between the experimental results, those corresponding to the models adopted in the literature, and the ones obtained in this study using CSTR model.

The results in Table 3 clearly show that the CSTR model correctly describes the behavior of the various industrial fluidized bed reactors studied, with differences from experimental results that are fairly acceptable, but slightly higher than those of (P-M models) of the literature. Table 3 also shows that the CSTR model describes these fluidized bed reactors better than the ADPF approach, allowing us to conclude that under high flow conditions, the fluidized bed reactor tends to exhibit CSTR rather than plug behaviour. According to this table, even though the CSTR approach describes the behavior of R2 and R3 fluidized bed reactors more accurately than the ADPF approach for the different conversions studied, we notice that the oxygen conversions predicted by the first model slightly underestimate the actual oxygen conversions. This can be explained by the fact that a small proportion of feed O_2 is involved in competitive oxidation reactions not taken into account in the model developed in this study. Indeed, only the main oxychlorination reaction was taken into account in the CSTR model used.

3.2 Effects of Operating Conditions on Converter Behavior

In this section, we have studied the effect of several operating parameters on installation behavior, using the CSTR model. We have also compared the curves obtained with those corresponding to the (P-M model) validated in the literature.

Figure 1 shows the evolution of ethylene conversion and catalyst bed temperature as a function of catalyst bed wall temperature. This figure also shows the results of the (P-M model) taken from the study by Khademi *et al*. [3]. The reactor and catalyst characteristics and feed operating conditions taken into account in the modeling and simulation correspond to the characteristics of the R4 reactor (Table 2). This figure shows that the reactor wall temperature has no noticeable effect on ethylene conversion, which is almost total. In fact, given the high reaction rate under the feed conditions studied, the reactor volume is more than sufficient for

near-total ethylene consumption. From the same figure, we can also observe that the temperature in the bed rises with the increase of the wall temperature. In fact, according to equation 29 corresponding to the heat balance on the reactor, the higher the wall temperature, the lower the heat flux to be evacuated by cooling, leading to this rise in reactor temperature. From a practical point of view, the reactor temperature must not exceed 513 K, to avoid competitive reactions leading to a drop in 1,2-dichloroethane selectivity [5].

Figure 2 shows the variation in ethylene conversion and reactor temperature with respect to feed temperature. The reactor and catalyst characteristics, wall temperature, feed molar flow rates and reactor pressure taken into account in the modeling and simulation also correspond with

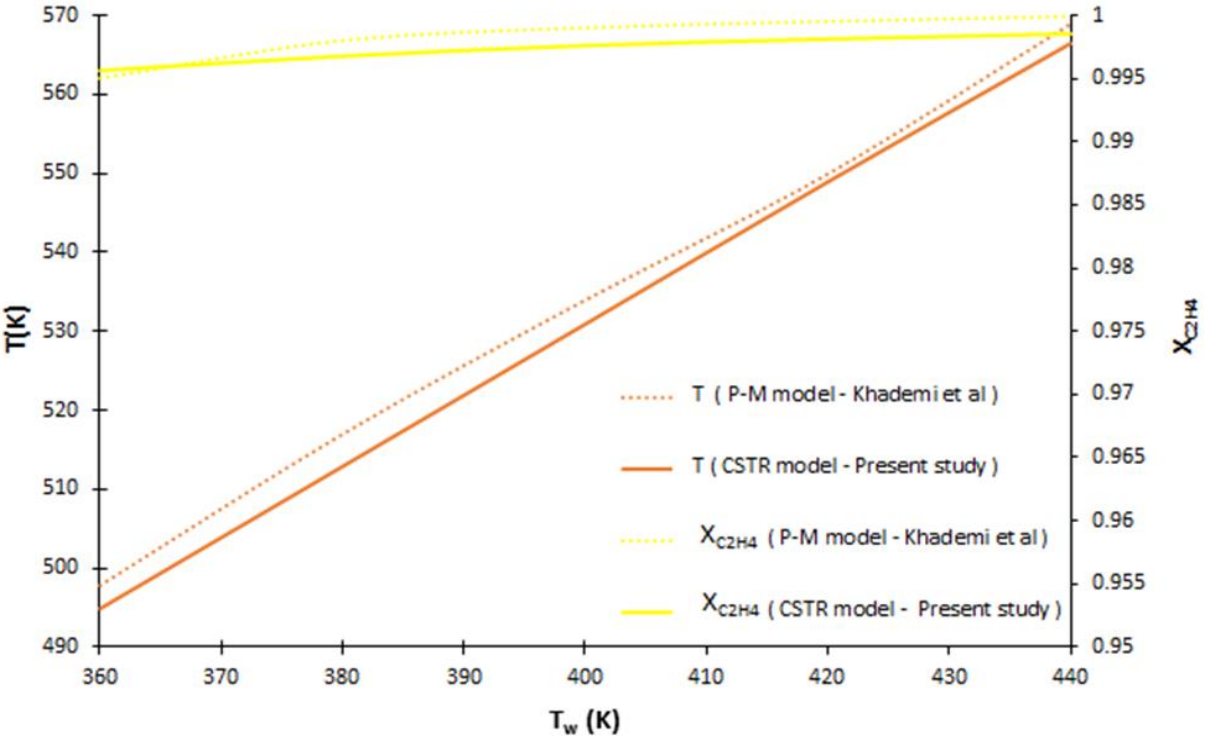

Figure 1. Effect of wall temperature on C_2H_4 conversion and bed temperature / comparison between the P-M model (literature) and the CSTR model (present study - Equations (21), (22), (29))

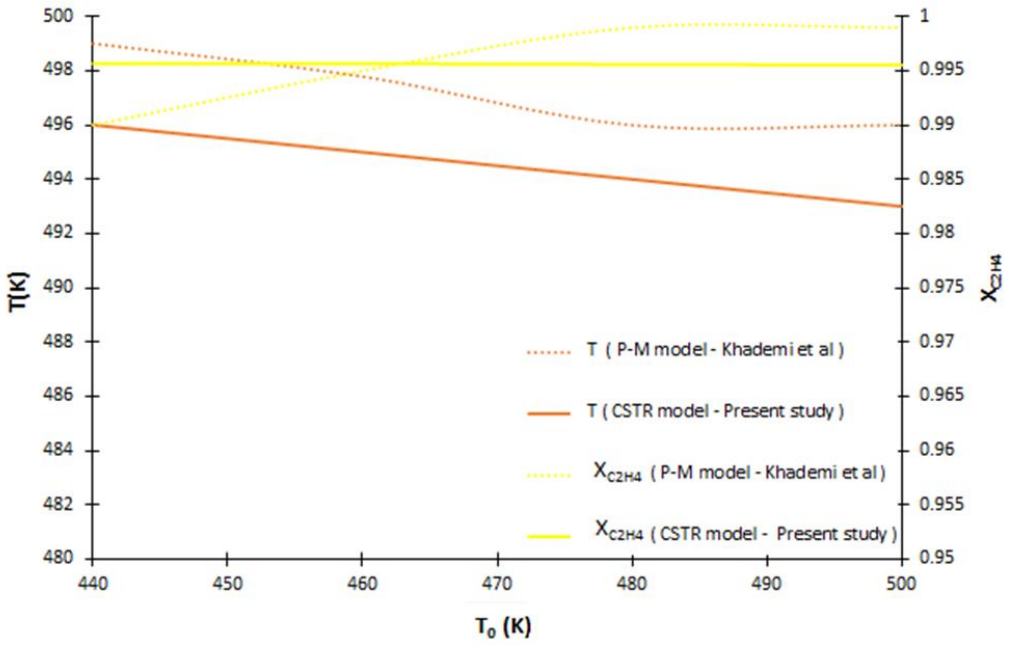

Figure 2. Effect of feed temperature on C_2H_4 conversion and bed temperature / comparison between the P-M model (literature) and the CSTR model (present study - Equations (21), (22), (29))

those of the R4 reactor. This figure also includes the results corresponding to the (P-M model) from the study by Khademi *et al*. [3]. Figure 2 shows that conversion to ethylene is almost complete at all feed temperatures, due to the high reaction rate under the feed conditions described above. Unlike the effect of wall temperature on reactor temperature, increasing feed temperature causes a slight drop in catalyst bed temperature. Indeed, the rise in feed temperature accelerates the near-total consumption of the limiting reactant, and thus causes an increasingly rapid pseudo-cancellation of the heat generation term (Equation (29)). This leads to a decrease in the temperature averaged over the entire reactor, and consequently to an increasing effect of the cooling temperature on the installation.

Figure 3 shows the effect of pressure on conversions of ethylene and hydrochloric acid. The feeding temperature and molar flow rates, the wall temperature (T_W), the reactor and catalyst characteristics taken into account in the CSTR modeling are still the same as for R4. Figure 3 also shows the results of the sensitivity analysis corresponding to the (P-M model) from the study by Khademi *et al.* [3]. This figure shows that the effect of pressure on reactants conversion is not noticeable. The slight rise in reactants conversion with increasing pressure can be explained by the rise in ethylene concentration, which can increase the oxychlorination reaction rate. Pressure can also affect the average voidage in the reactor via its effect on the density of the gas mixture.

Figure 4 shows the effect of ethylene molar percentage in the feed on hydrochloric acid, ethylene and oxygen conversions. The feed and wall temperatures, feed molar flow rates of hydrochloric acid and oxygen, pressure and

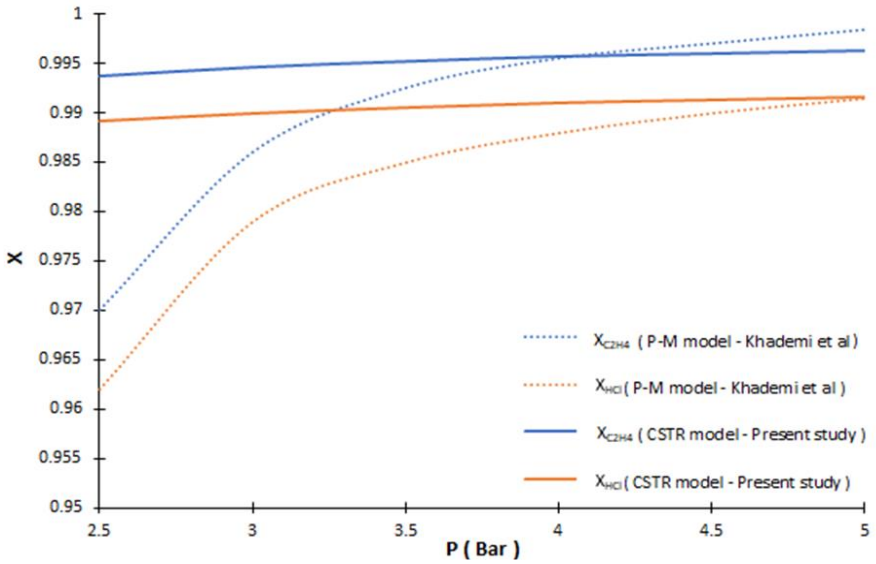

Figure 3. Effect of pressure on C_2H_4 and HCl conversions / comparison between the P-M model (literature) and the CSTR model (present study - Equations (21), (22), (29))

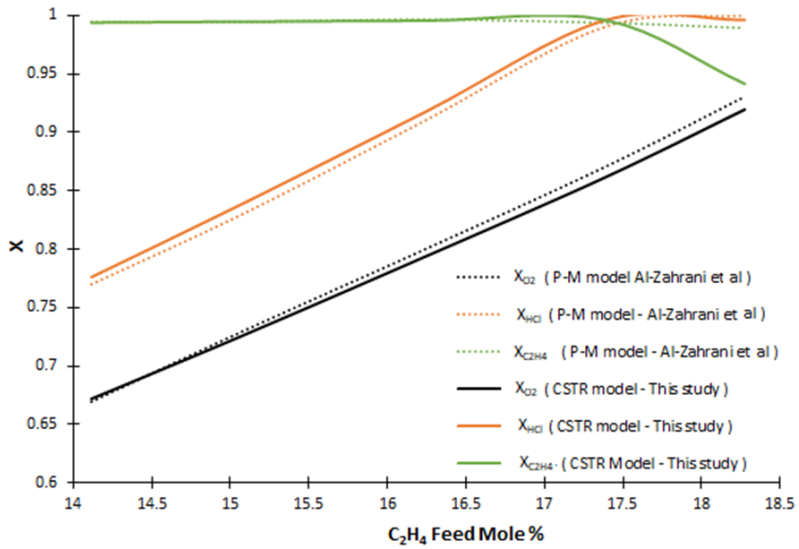

Figure 4. Effect of C_2H_4 mole fraction on reactants conversion / comparison between the P-M model (literature) and the CSTR model (present study - Equations (21), (22), (29))

reactor and catalyst characteristics taken into account in the modeling and simulation correspond in this case to that of R1 (Table 2). Figure 4 also shows the results of the (P-M model) from the study by Al-Zahrani *et al*. [7]. According to this Figure 4, ethylene conversion is almost complete when the ethylene feeding mole fraction is below 17.38%. Indeed, as discussed above, given the high reaction rate under these feed conditions, the reactor volume is amply sufficient for the total consumption of C_2H_4. Under these conditions, ethylene is the limiting reactant, and increasing its fraction in the feeding leads to increased conversions of the other reactants (O_2, HCl). In fact, the degree of advancement of the reaction rises as the flow rate of the limiting reactant increases. When the fraction of C_2H_4 in the feeding exceeds 17.38%, hydrochloric acid becomes the limiting reactant, and the degree of advancement of the reaction is fixed at the molar flow rate of HCl feed divided by -αHCl. Therefore, any increase in C_2H_4 feeding has no effect on X_{HCl} and leads to a decrease in X_{C2H4}. Under the feeding conditions considered, oxygen is always fed in excess, this is what explain the increase in its conversion with increasing feed flow rate of the limiting reactant.

The two approaches (P-M model) and (CSTR model) are in agreement on the stirred reactor behavior of the reaction phase containing the entire catalytic mass. The former considers the presence of a plug phase (bubble) exchanging material and heat with the reaction phase (emulsion), while the latter assumes that the entire installation is a continuous stirred reactor. Thus, the good agreement between the results of these two models, which can be seen in Figures (1-4), may be the consequence of the first approach's consideration of rapid mass and heat transfer between the bubble phase and the emulsion phase under the operating conditions studied.

3.3 Evaluation of the Reactor Behavior under Low-Flow Rate Conditions using the (P-P Model)

In this section, the behavior of the reactor when the feeding flow rate is not very high ($U_{mb} \leqslant U_0 \leqslant 6.U_{mf}$) and when the reactor is long (L/D $\geqslant$10) is studied by adopting the P-P approach since it is the most suitable under these conditions [14,28]. The characteristics of the reactor, catalyst and feed stream are presented in Table 4. Under these conditions, calculation of the minimum bubbling velocity (U_{mb}) using the formula (Eq. (20)) presented in Table 1 led to the conclusion that U_{mb} not exceed 2.69 U_{mf}.

The length and diameter of the reactor and the molar flow rate feeding the reactor are chosen in such a way that the conditions relating to geometric characteristics and superficial velocity presented at the top of this section are met. The chosen catalyst characteristics correspond perfectly to the commercial catalysts used for this reaction [3,7]. On a large scale, the reaction is almost complete, so a ratio of (C_2H_4)/HCl = 0.5 is chosen to ensure high X_{HCl} without C_2H_4 losses [7]. From a practical point of view, it is recommended to opt for an O_2/HCl ratio in the range 0.3-0.75 to avoid catalyst deactivation [40], hence the value of 0.5 corresponding to this ratio has been chosen. The choice of a high fraction of N_2 in the feeding is also motivated by experimental reasons. In fact, the high flow rate of this inert gas in the gas mixture attenuates thermal hot spots and reactor defluidization caused by the extreme exothermicity of the reaction [2]. This avoids the disastrous effects of such phenomena on the catalyst, on the selectivity of 1,2-dichloroethane and on the gas-solid mixture [2,5].

Table 2. Model Input and Reactor Parameters for different Industrial Oxychlorination Fluidized-Bed Reactors

Parameter	Reactor 1 [R1] Al-Zahrani *et al.* [7]	Reactor 2 [R2] Montbelli *et al.* [5]	Reactor 3 [R3] Montbelli *et al.* [5]	Reactor 4 [R4] Khademi *et al.* [3]
Bed height at minimum fluidization (m)	7	6.83	6.3	7
Bed diameter (m)	3.4	2.76	4.05	3.4
Catalyst particle density (kg.m^{-3})	1369	1520	1520	1369
Catalyst particle diameter (μm)				
Bed pressure (Pa)	80	50	50	80
Feed temperature (K)				
Cooling medium temperature (K)	400000	470000	510000	400000
Emulsion temperature (K)	460			460
Feed molar flow rate of HCl/C_2H_4/O_2 (mol.s^{-1})	360			360
		504	508.5	
	64/32/ 18.5	81.97/45.08/ 23.48	197.43/102.66/ 60.75	64/31.85/21.5

Th sensitivity analysis presented in Figures (5-10) has allowed to evaluate the effect of feeding temperature, wall temperature and feeding flow rate on the converter behavior when the (P-P model) is used. Figure 5 shows the effect of different feeding temperatures listed in Table 4 on the thermal profile in the reactor for U_0=6.U_{mf}, T_W=500 K and for the other feeding, reactor and catalyst characteristics presented in this table. From this figure, it is clear that the thermal hot spots are located at the reactor inlet and in the emulsion phase, since it is in this position of the converter that the highest concentrations of ethylene are found, and it is in this phase that the catalyst is exclusively located. Under these conditions, the reaction rate is high, and so the heat flux released by the reaction is significant (see Equation (40)). In the rest of the reactor, these hotspots disappear and the temperature of the emulsion phase takes on the value of T_w, because with the drop in C_2H_4 concentration in this phase in the rest of the converter, the heat production term for the chemical reaction in Equation (40) becomes very low, and the term corresponding to the heat flux subtracted by cooling (Equation (40)) becomes dominant. Figure 5 also shows that the higher the feed temperature, the weaker the hot spots. Indeed, the higher the feeding temperature, the higher the emulsion volumetric flow rate at (Z=0), so the C_2H_4 concentration drops at the reactor inlet, which implies a drop in the reaction rate and therefore in the term of heat release by reaction present in equation 40, and this is reflected in the drop in hot spots at the inlet as T_0 increases. Finally, from this figure, the bubble temperature takes on the feeding temperature at the reactor inlet, gradually moving towards the temperature value imposed by the wall (T_W) and reaching it at increasingly greater longitudinal positions as the temperature difference between feeding and wall temperature (T_W) increases. In fact, the greater this difference, the greater the length required to achieve thermal equilibrium and stop heat transfer between the two phases.

Figure 6 shows the profile of X_{C2H4} along the installation for the same conditions as those corresponding to Figure 5. This figure shows that there is a significant rise in X_{C2H4} at the reactor inlet from (0 to 0.2) and this phenomenon is

Table 3. Comparison between experimental data, literature models and CSTR model predictions RE: Relative error compared to the plant results

Literature study	Outlet data	Plant	CSTR model-Present study	Literature model	RE (%) for CSTR model-Present Study	RE (%) for the literature model
Al-Zahrani *et al.* (P-M model) [7] R1	HCl conversion	0.983	0.996	0.985	1.34	0.25
	C_2H_4 conversion	0.993	0.996	0.994	0.32	0.13
	Outlet temperature (K)	498	497	498.18	-0.2	0.04
Montbelli *et al.* (ADPF model) [5] R2	HCl conversion	0.992	1	0.963	0.84	-2.92
	C_2H_4 conversion	0.912	0.909	0.893	-0.34	-2.06
	O_2 conversion	0.952	0.873	0.852	-8.34	-10.55
Montbelli *et al.* (ADPF model) [5] R3	HCl conversion	0.996	1	0.953	0.83	-4.27
	C_2H_4 conversion	0.962	0.962	0.930	-0.03	-3.28
	O_2 conversion	0.920	0.812	0.785	-11.71	-14.65
Khademi *et al.* (P-M) Model [3] R4	HCl conversion	0.983	0.991	0.988	0.81	0.5
	C_2H_4 conversion	0.993	0.996	0.995	0.27	0.25
	Outlet temperature (K)	498	495	497.79	-0.6	-0.04

Table 4. Model Input and Parameters for reactor operating at low flows

Parameter	Value
Bed height at minimum fluidization (m)	1.6
Bed diameter (m)	0.04
Catalyst particle density (kg.m^{-3})	1369
Catalyst particle diameter (µm)	80
Bed pressure (Pa)	400000
Feed temperature (K)	400-460-480
$\frac{U_0}{U_{mf}}$	3.22-4-6
Wall temperature (K)	473-500-530
feed mole fraction of $HCl/C_2H_4/O_2$ in reactant flow rate	0.5/0.25/0.25
Molar flow rate of N_2 (mol.s^{-1})	17.92.10^{-4}

similar for the three T_0 studied. In fact, this result is the consequence of the thermal hot spots and high ethylene concentrations in emulsion phase at the installation inlet causing high reaction rate and consumption of high quantities of C_2H_4, resulting in this peak in the ethylene conversion, which is significant despite the resistance to transfer phenomena. This figure shows also that the effect of variation of feeding temperature from 400 K to 480 K on X_{C2H4} is less important than that on the thermal profile in the reactor. This is because the process is controlled by mass transfer between the two phases studied, which is less sensitive to temperature than the actual chemical reaction, whose effect of temperature on its rate is greater. In fact, due to the limitations of mass transfer between phases, the emulsion phase only receives small flows of C_2H_4 from the bubble phase, which is richer in this reactant. So, although temperature variation may affect C_2H_4 consumption in the emulsion phase, this will not be reflected in the conversion profile, since the bulk of this species is localized in the bubble phase (see Equation (41)).

Figure 7 shows the effect of different wall temperatures listed in Table 4 on the thermal profile in the reactor for T_0 = 460 K, for the same molar flow rates and for the same catalyst and reactor characteristics presented at the head of the paragraph. From this figure, we can see that

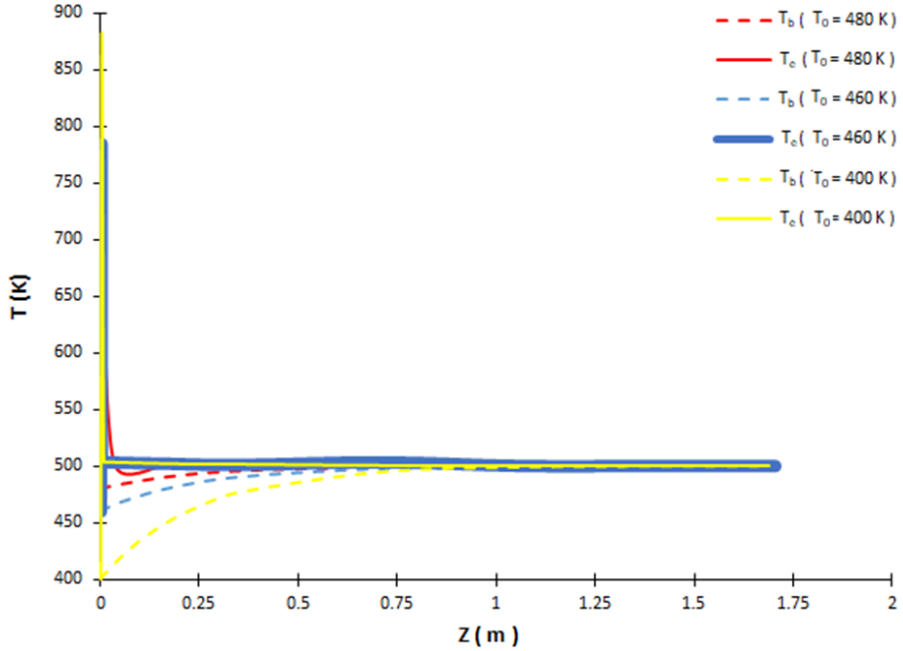

Figure 5. Effect of feed temperature on bubble and emulsion temperature profiles / P-P model (Equations (34)-(35), (38)-(40))

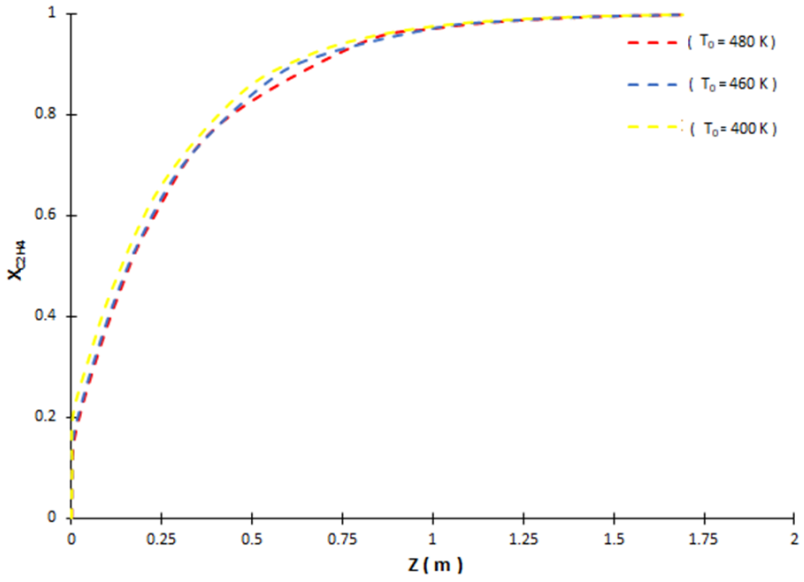

Figure 6. Effect of feed temperature on C_2H_4 conversion profile / P-P model (Equations (34)-(35), (38)-(41))

the hot spots at the reactor inlet for the emulsion phase become increasingly important as the wall temperature (T_W) rises. Indeed, the higher the T_W, the smaller the difference between this temperature and the temperature of the emulsion phase at the reactor inlet. This leads to a weakening of the heat extracted by cooling term in equation 40, which in turn leads to a rise in the temperature of the emulsion at the reactor inlet, reflected in the rise in hot spots. The presence of the hot spots at the reactor inlet in the emulsion phase is explained by the same reasons as given for this phenomenon in the interpretation of the curves in Figure 5. As with the latter, the temperature of the bubble is T_0 at $z = 0$, reaching T_W at a longitudinal position whose value increases as the temperature difference between the feed and the wall rises. This result is interpreted using the same justifications we adopted to explain this phenomenon, which can also be seen in the curves of Figure 5.

For the same conditions as in Figure 7, Figure 8 shows the profile of X_{C2H4} along the installation. The curves in this figure are similar to those in Figure 6. To interpret the curves in this new figure, we can then give the same explanations adopted to justify the X_{C2H4} peaks at the converter inlet and the lacking effect of temperature

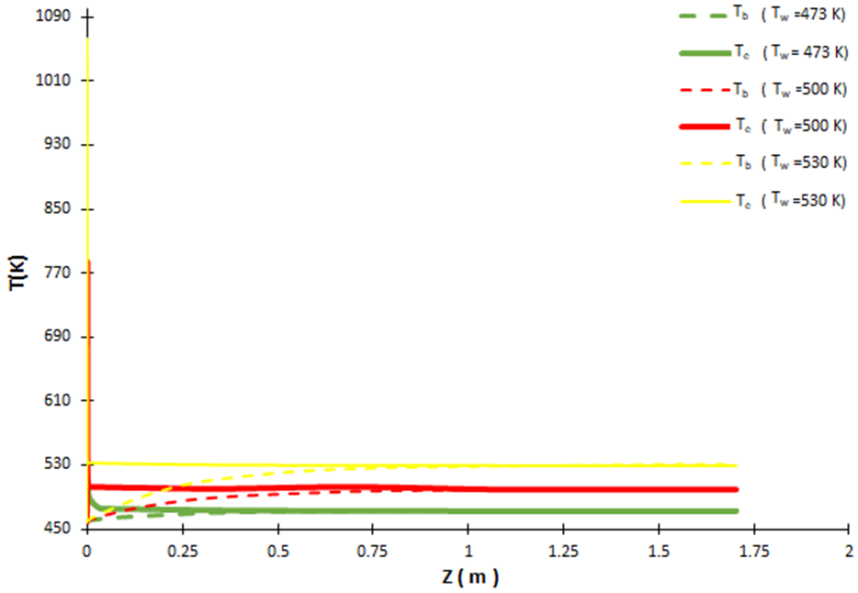

Figure 7. Effect of wall temperature on bubble and emulsion temperature profile / P-P model (Equations (34)-(35), (38)-(40))

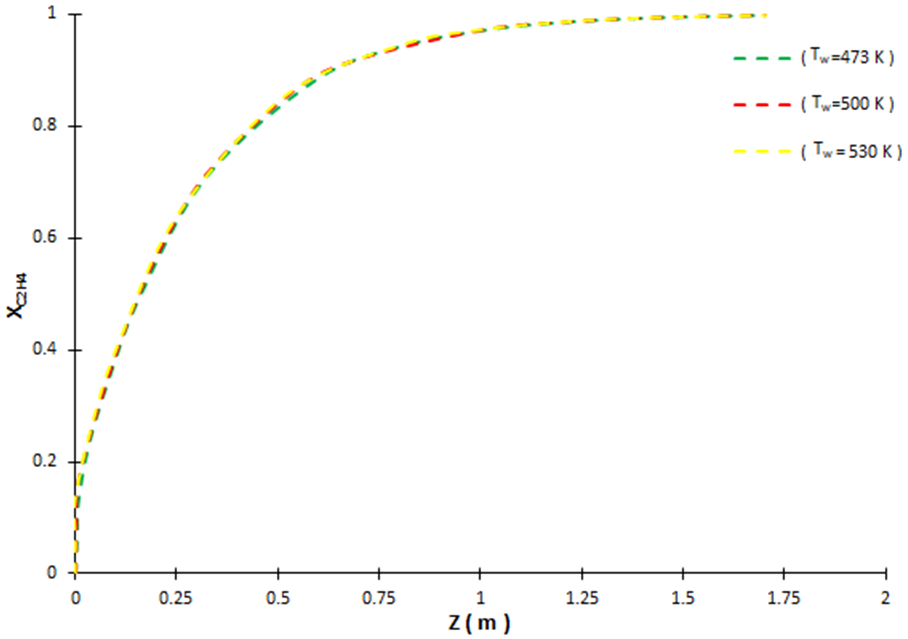

Figure 8. Effect of wall temperature on C_2H_4 conversion profile / P-P model (Equations (34)-(35), (38)-(41))

variation on the X_{C2H4} profile shown in the curves in Figure 6.

Figure 9 shows the effect of different feeding superficial velocities listed in Table 4, corresponding to various reactant inlet flow rates, on the thermal profile in the reactor for T_0 = 460 K, for T_W = 500 K and for the other characteristics of feeding, reactor and catalyst shown in this table. According to this figure, the higher the superficial velocity, the higher the hot spot at the reactor inlet in the emulsion phase. In fact, given that the molar flow rate of N_2 is fixed in all the simulations presented in this paragraph, increasing the superficial velocity of feed implies an increase in the concentration of reactants and, in particular, an increase in the concentration of C_2H_4, which leads to an acceleration of the reaction rate and, consequently, an increase in the heat release by chemical reaction term in equation 40, manifested by this increase in hot spots in the emulsion phase. In the bubble phase, this figure shows the presence of temperature profiles between the two phases, which are influenced less by variations in inlet superficial velocities than by temperature differences between phases. In fact, as previously discussed, the thermal profile in the bubble phase depends only on the temperature difference between the bubble phase at the inlet (feed temperature) and the temperature of the emulsion phase in the rest of the converter (wall-imposed temperature). Since these two temperatures are maintained for the three simulations shown in Figure 9, this profile is not influenced. Figures 5, 7, and 9 show that by acting either on the feeding temperature, on the wall temperature or on the reactant flow rate, it is possible to control hot spots and attenuate them, enabling their negative effects on the catalyst and on the selectivity of 1,2-dichloroethane.

Figure 10 shows the profile of X_{C2H4} along the installation for the same conditions as described in Figure 9. The X_{C2H4} peaks seen at the installation inlet are explained by the same reasons given for the explanation of this phenomenon in the curves of Figures 6 and 8. We also note that the lower the superficial velocity at

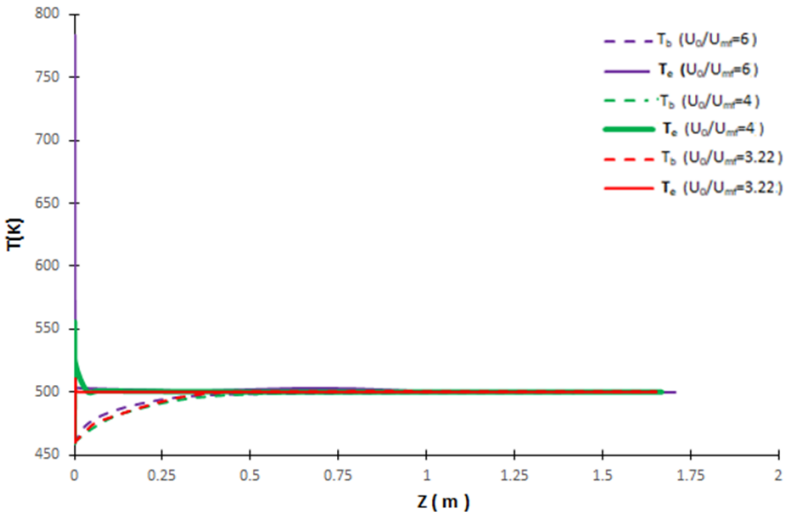

Figure 9. Effect of inlet superficial velocity on bubble and emulsion temperature profiles / P-P model (Equations (34)-(35), (38)-(40))

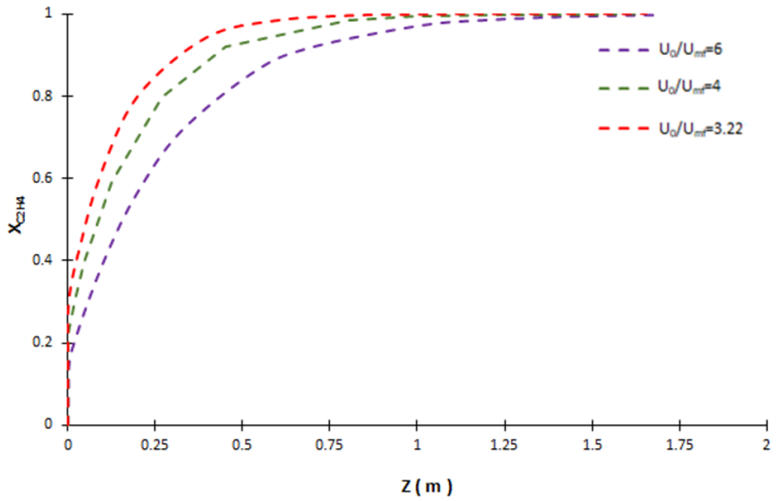

Figure 10. Effect of inlet superficial velocity on C_2H_4 conversion profile / P-P model (Equations (34)-(35), (38)-(41))

the reactor inlet, the greater the intensity of these peaks (0.3 for U_0/U_{mf} = 3.22 and 0.2 for U_0/U_{mf} = 6) and the total consumption of C_2H_4 is achieved at more backward positions in the reactor. In fact, the lower the U_0, the lower the molar flow rate of reactants, so the conversion of reactants by catalytic mass is greater, and the total transformation of limiting reactants into products requires less catalyst and less reaction volume.

3.4 Comparison between (P Model) and (P-P Model) under Low Flow Conditions

Approach (P) is studied in this section in order to evaluate the behavior of the converter in the absence of limitations to the transfer phenomena between the bubble and the emulsion. Figure 11 shows the effect of different feeding superficial velocity on the thermal profile in the reactor for T_0 = 460 K, for T_W = 500 K and for the other reactor and catalyst feeding characteristics presented in Table 4, adopting the (P) and (P-P) approaches. According to this figure, the hot spots in the bed corresponding to the (P model) are rather close to those relating to the (P-P) emulsion phase, this result is valid for both superficial velocities examined. Indeed, the conditions at the reactor inlet of the plug approach correspond well to the ones present in the emulsion phase (P-P model) at that converter inlet in terms of chemical species concentrations and in terms of catalyst mass. This implies, then, that the chemical reaction heat release terms divided by reactor volume from Equation (33) ($-\Delta H_r.r_{C2H4Cl2}.(1-\varepsilon_{moy})$) and the term corresponding to this energy release divided by emulsion phase volume from Equation (40) ($-\Delta H_r.r_{C2H4Cl2}.(1-\varepsilon_{mf}).(1-\delta)$) are identical at (z = 0), which explains the pseudo-overlap between the hot spots for the two models studied. For the plug model, after the hot spot, the temperature maintained along the rest of the reactor is the temperature of the wall (T_W). This is because all the limiting reactant is consumed at the reactor inlet, which means that the term of heat released by reaction in Equation 33 is cancelled out throughout the rest of the installation, and the prevailing temperature is therefore the one maintained by the wall. The descriptions and interpretations of the thermal profiles relative to the (P-P model) have already been detailed and discussed in the preceding paragraphs.

Figure 12 shows the evolution of X_{C2H4} along the reactor for the same conditions as in Figure 11. This figure highlights the effect of limitations of mass transfer between phases on reactor

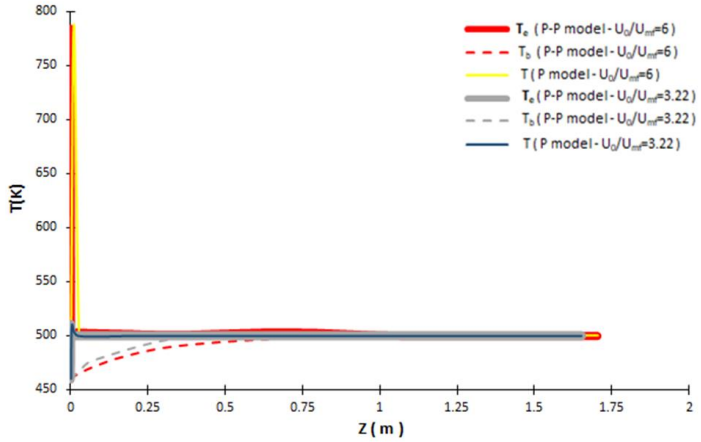

Figure 11. Effect of inlet superficial velocity on reactor thermal profile for (P) and (P-P) models (Equations (32)-(34) (P) and Equations (34)-(35), (38)-(40) (P-P))

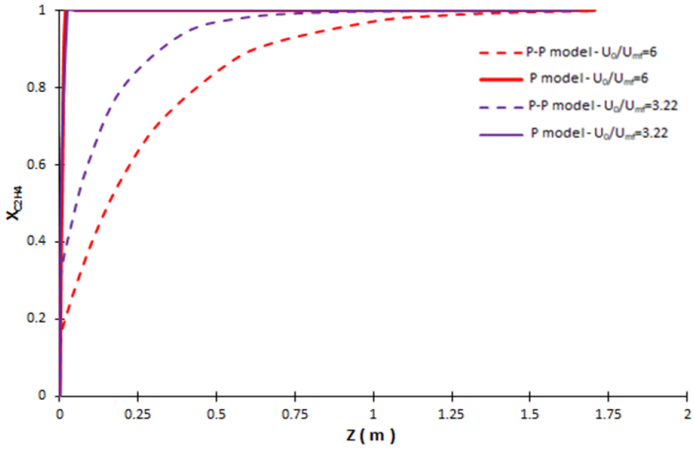

Figure 12. Effect of inlet superficial velocity on C_2H_4 conversion for (P) and (P-P) models (Equations (32)-(34) (P) and Equations (34)-(35), (38)-(41) (P-P))

behavior. Indeed, in the absence of these (P model), all C_2H_4 is converted at the reactor inlet. Because of these interphase mass transfer resistances, almost half the reactor volume is required for total C_2H_4 consumption if U_0/U_{mf} = 3.22, and almost 80% of the reactor is needed to achieve total C_2H_4 consumption if U_0/U_{mf} = 6.

4. Conclusions

The present study revealed that the CSTR approach can correctly predict the behavior of industrial fluidized beds for ethylene oxychlorination characterized by a turbulent regime, given the good agreement between the simulation results corresponding to the CSTR model and the results corresponding to several fluidized-bed converters dedicated to this oxychlorination. It was also demonstrated that the sensitivity analysis results for this model are quite close to those of the (P-M) approach validated in many studies in the literature. Predicting the behavior of these fluidized bed reactors under low flow conditions ($U_0 \leqslant 6.U_{mf}$-bubbling regime) by adopting the P-P approach showed that under these conditions, thermal hot spots with significant peaks are indeed present at the converter inlet. In addition, solutions for controlling this phenomenon by adjusting several operating parameters (T_0, T_W, U) were proposed. Finally, a comparison of the (P-P) approach with the (P) one highlighted the significant impact of limitations to transfer phenomena on the process under these conditions.

Acknowledgments

The authors would like to acknowledge the Moroccan Ministry of Higher Education, Scientific Research and Innovation.

CRediT Author Statement

Author contributions: W. El Bazi: Conceptualization, Methodology, Software, Supervision; W. El Bazi, M. Bideq, A. Abidi and S. Yadir: Formal Analysis, Invistigation, Ressources, Commentary or revision; W. El Bazi, M. Bideq and A. Abidi : Writing - Review & Editing. All authors have read and agreed to the published version of the manuscript.

References

[1] Syed, I., Ray, S.D. (2014). *Encyclopedia of Toxicology*. (Third Edition). Bethesda, MD: Academic Press.

[2] Kang, S.G., Yun, K., Sung, R.S., Sang, D.K. (2010). 1,2-Dichloroethane production by two-step oxychlorination reactions in a fluidized bed reactor. *Chemical Engineering Science*, 65, 499 – 503. DOI: 10.1016/j.ces.2009.02.052.

[3] Khademi, M.H., Taghavi, A. (2017). Optimization of ethylene oxychlorination fluidized-bed reactor using Differential Evolution (DE) method. *Scientia Iranica C*, 24, 1253-1263. DOI: 10.24200/SCI.2017.4109.

[4] Moradi, Z., Farsi, M. (2020). Simulation of direct chlorination of ethylene in a two-phase reactor by coupling equilibrium, kinetic and population balance models. *Chem. Prod. Process Model*, 20200061, 1-13. DOI : 10.1515/cppm-2020-0061.

[5] Montebelli, A., Tronconi, E., Orsenigo, C., Ballarini, N. (2015). Kinetic and Modeling Study of the Ethylene Oxychlorination to 1,2-Dichloroethane in Fluidized-Bed Reactors. *Industrial & Engineering Chemistry Research*, 54, 9513-9524. DOI: 10.1021/acs.iecr.5b01456.

[6] Moreira, J.C.S., Pires, C.A.M. (2010). Modelling and Simulation of an Oxychlorination Reactor in a Fluidized Bed. *The Canadian Journal Of Chemical Engineering*, 88, 350-358. Doi : 10.1002/cjce.20281.

[7] Al-Zahrani, S.M., Aljodai, A.M., Wagialla, K.M. (2001). Modelling and simulation of 1,2-dichloroethane production by ethylene oxychlorination in fluidized-bed reactor. *Chemical Engineering Science*, 56, 621-626. DOI: 10.1016/S0009-2509(00)00268-2.

[8] Faghih, S.M., Kianfar, E. (2018). Modeling of Fluid Bed Reactor of Ethylene Di Chloride Production in Abadan Petrochemical Based on Three-Phase Hydrodynamic Model. *International Journal of Chemical Reactor Engineering*, 20180006, 1-14. DOI: 10.1515/ijcre-2018-0006.

[9] El Bazi, W., Bideq, M., El Abidi, A., Yadir, S., Ouartassi, B. (2022). Numerical study of a water gas shift fxed bed reactor operating at low pressures. *Bull Chem Reaction Eng Catal*, 17, 304–321. DOI: 10.9767/bcrec.17.2.13510.304-321.

[10] El Bazi, W., Bideq, M., Yadir, S., El Abidi, A. (2023). Efects of catalyst distribution, particle geometry, and process conditions on the behavior of a water gas shift reactor under moderate pressures: a modeling study. *Reaction Kinetics, Mechanisms and Catalysis*, 136, 1859-1890. DOI: 10.1007/s11144-023-02431-x.

[11] McAuley, K.B., Talblot, J.P., Harris, T.J. (1994). A comparaison of two-Phase and well-mixed models for fluidized-bed polyethylene reactors. *Chemical Engineering Science*, 49, 2035-2045. DOI: 10.1016/0009-2509(94)E0030-T.

[12] Mostoufi, N., Cui, H., Chaouki, J. (2001). A Comparison of Two- and Single-Phase Models for Fluidized-Bed Reactors. *Ind. Eng. Chem. Res.*, *40,* 5526-5532. DOI: 10.1021/ie010121n.

[13] Fernandes, F.A.N., Lona, L.M.F. (2001). Fluidized-bed reactor modeling for polyethylene production. *Journal of Applied Polymer Science*, 81, 321–332. DOI: 10.1002/app.1442.

[14] Lu, W., Teng, L., Xiao, W. (2003). Theoretical Analysis of Fluidized-Bed Reactor for Dimethyl Ether Synthesis from Syngas. *Int. J. Chem. React. Eng.*, 1, 1-10. DOI: 10.2202/1542-6580.1086.

[15] Shaofen, L. (2016). *Reaction Engineering*. Edition. Butterworth-Heinemann.

[16] Wagialla, K.M., Elnashaie, S. S. E. H. (1991). Fluidized-Bed Reactor for Methanol Synthesis. A Theoretical Investigation. *Ind. Eng. Chem. Res.*, 30, 2298-2308. DOI: 10.1021/ie00058a009.

[17] Fakeeha, A.H., Wagialla, K.M., AI-Shriahy, F.A. (1992). Modelling and Simulation of Acrylonitrile Synthesis from Propylene Using Fluidized Bed Technology. *J. King Saud Univ.*, 4, 127-142. DOI: 10.1016/S1018-3639(18)30560-9.

[18] Jafari, R., Sotudeh-Gharebagh, R., Mostoufi, N. (2004). Modular Simulation of Fluidized Bed Reactors. *Chem. Eng. Technol.*, 27, 123-129. DOI: 10.1002/ceat.200401908.

[19] Hamzehei, M., Rahimzadeh, H., Ahmadi, G. (2010). Computational and Experimental Study of Heat Transfer and Hydrodynamics in a 2D Gas-Solid Fluidized Bed Reactor. *Ind. Eng. Chem. Res.*, 49, 5110–5121. DOI: 10.1021/ie900510a.

[20] Singh, R.I., Brink, A., Hupa, M. (2013). CFD modeling to study fluidized bed combustion and gasification. *Applied Thermal Engineering*, 52, 585-614. DOI: 10.1016/j.applthermaleng.2012.12.017.

[21] Julián, I., Herguido, J., Menéndez, M. (2014). CFD model prediction of the Two-Section Two-Zone Fluidized Bed Reactor (TS-TZFBR). *Hydrodynamics*, 248, 352-362. DOI: 10.1016/j.cej.2014.03.028.

[22] Wachi, S., Asai, Y. (1994). Kinetics of 1,2 Dichloroethane formation from ethylene and cupric chloride. *Industrial Engineering and Chemistry Research*, *33*, 259-264. DOI: 10.1021/IE00026A013.

[23] Carrubbba, R.V., Spencer, J.L. (1970). Kinetics of the Oxychlorination of Ethylene. *Ind. Eng. Chem. Process Des. Develop.*, 9, 414-419. DOI: 10.1021/I260035A009.

[24] Farsi, M., Salimi, M. (2021). Modeling and Optimization of Ethylene Oxychlorination Fluidized Bed Reactor in Arvand Petrochemical Complex. *Nashrieh Shimi va Mohandesi Shimi Iran (NSMSI)*, 40, 213-224. DOI: 20.1001.1.10227768.1400.40.3.18.7.

[25] Junsittiwate, R., Kodchakong, A., Srinophakun, T.R. (2018). Ethylene Dichloride Production by Oxychlorination in a Fluidized Bed Reactor with CFD Model. *Asian Journal of Applied Sciences*, 6, 245-258. DOI: 10.24203/ajas.v6i5.5506.

[26] Botero, A.M., Grace, J.R., Elnashaie, S.S.E.H., Lim, C.J. (2009). Advances in Modeling of Fluidized-Bed Catalytic Reactors: A Comprehensive Review. *Chem. Eng. Comm.*, 196, 1375–1405. DOI: 10.1080/00986440902938709.

[27] Toei, R., Oichi, M., Hayashi, H., Kubo, K., Yanagida, T., Mastuno, R. (1977). Hydrogenation of ethylene in two-dimensional gas-solid fluidized bed with perforated plate. *Journal of Chemical Engineering of Japan*, 10, 307-313. DOI: 10.1252/jcej.10.307.

[28] Davidson, J.F. (1991). Communication, The Two-phase Theory of Fluidization: Successes and Opportunities. In *AIChE Symp. Ser.*, 87, 1-12. Houston. AIChE Symp.

[29] Magistro, A.J, Cowfer, J.A. (1986). Real world of industrial chemistry: Oxychlorination of ethylene. *J. Chem. Educ.*, 63, 1056-1058. DOI: 10.1021/ED063P1056.

[30] Toor, F.D., Calderbank, P.H. (1968). Communication, Performance of an 18 in diameter fluidised-bed catalytic reactor with a pseudo first-order reaction and discussion of scale-up problems. *In Proceedings of the Tripartite Chemical Engineering Conference*,12-20. Montreal. The tripartite chemical engineering conference.

[31] Maklavany, D.M., Shariati, A., Nikou, M.R.K., Roozbehani, B. (2017). Hydrogen Production via Low Temperature Water Gas Shift Reaction: Kinetic Study, Mathematical Modeling, Simulation and Optimization of Catalytic Fixed Bed Reactor using gPROMS. *Chemical Product and Process Modeling*, 12, 20160063. DOI: 10.1515/cppm-2016-0063.

[32] Khraibet, S.A, Mazloom, G., Banisharif, F. (2021). Comparative Study of Different Two-Phase Models for the Propane Oxidative Dehydrogenation in a Bubbling Fluidized Bed Containing the VOx/γ-Al_2O_3 Catalyst. *Ind. Eng. Chem. Res.*, 60, 9729-9738. DOI: 10.1021/acs.iecr.1c01040.

[33] Shamiri, A., Hussain, M.A., Mjalli, F.S., Shafeeyan, M.S., Mostoufi, N.(2014). Experimental and Modeling Analysis of Propylene Polymerization in a Pilot-Scale Fluidized Bed Reactor. *Ind. Eng. Chem. Res.*, 53, 8694-8705. DOI: 10.1021/ie501155h.

[34] Singh, R.K., Roy, G.K. (2005). Prediction of minimum bubbling velocity, fluidization index and range of particulate fluidization for gas–solid fluidization in cylindrical and non-cylindrical beds. *Powder Technology*, 159, 168-172. DOI: 10.1016/j.powtec.2005.08.008.

[35] Perry, R.H., Green, D.W., Maloney, J.O., Abbott, M.M., Ambler, C.M., Amero, R.C. (1997). *Perry's Chemical Engineers' Handbook*. Edition. New York: McGraw-Hill.

[36] Villermaux, J. (1993). *Génie de la réaction chimique*. Edition. Paris: Tec & Doc-Lavoisier.

[37] Levenspiel, O. (1999). *Chemical Reaction Engineering*. Edition. New York: John Wiley & Sons.

[38] Constantinides, A., Mostoufi, N. (1999). *Numerical Methods for Chemical Engineers with MATLAB Applications*. Edition. New Jersey: Prentice Hall PTR.

[39] Lu, W.Z., Teng, L.H., Xiao, W.D. (2004). Simulation and experiment study of dimethyl ether synthesis from syngas in a fluidized-bed reactor. *Chemical Engineering Science*, 59, 5455–5464. DOI: 10.1016/j.ces.2004.07.031.

[40] Pan, H.Y., Minet, R.G., Benson, S.W., Tsotsis, T.T. (1994). Process for converting hydrogen chloride to chlorine. *Ind. Eng. Chem. Res.*, 33, 2996-3003. DOI: 10.1021/ie00036a014